

# Alteration in the expression of inflammatory parameters as a result of oxidative stress produced by moderate zinc deficiency in rat lung

Verónica S. Biaggio, María V. Pérez Chaca, Susana R. Valdéz, Nidia N. Gómez, and María S. Gimenez

*Departamento de Bioquímica y Ciencias Biológicas. Facultad de Química, Bioquímica y Farmacia, Universidad Nacional de San Luis–IMIBIO–CONICET, San Luis, Argentina*

## ABSTRACT

Suboptimal intake of dietary zinc (Zn) is one of the most common nutritional problems worldwide. Previously, the authors have shown that zinc deficiency (ZD) produces oxidative and nitrosative stress in lung of male rats. The goal of this study is to test the effect of moderate ZD on insulin-like growth factor (IGF)-1, IGF-binding protein (IGFBP)-5, NADH oxidase (NOX)-2, tumor necrosis factor alpha (TNF $\alpha$ ), as well as the effect of restoring zinc during the refeeding period. Adult male rats were divided into 3 groups: Zn-adequate control group, Zn-deficient group, and Zn-refeeding group. eNOS, metallothionein (MT) II, and NOX-2 was increased in ZD group. The authors observed an increased gene transcription of superoxide dismutase (SOD)-2 and glutathione peroxidase (GPx)-1 in ZD group, as well as in ZD-refeeding group, but catalase (CAT) transcription did not change in the treated groups. Proinflammatory factors, such as TNF $\alpha$  and vascular cell adhesion molecular (VCAM)-1 increased in ZD, whereas it decreased in ZD refeeding. However, peroxisome proliferator-activated receptor gamma (PPAR $\gamma$ ) and IGF-1 gene transcription decreased in ZD, whereas IGFBP-5 decreased in the ZD group. These parameters are associated to alterations in the lung histoarchitecture. The zinc supplementation period is brief (only 10 days), but it is enough to inhibit some proinflammatory factors. Perhaps, zinc deficiency implications must be taken into account in health interventions because inflammation and prooxidant environment are associated with ZD in lung.

**KEYWORDS** catalase; endothelial nitric oxide synthase; glutathione peroxidase; insulin growth factor binding protein-5; insulin growth factor-1; NADPH oxidase-2; peroxisome proliferator-activated receptor gamma; superoxide dismutase; tumor necrosis factor alpha; vascular cell adhesion molecule-1

Zinc is an essential nutrient and one of the most abundant biological trace metals. It also has special roles in the conducting airways. It has been shown

that zinc deficiency increases oxidative damage in the airways by infiltration of inflammatory cells and increased oxidative and nitrosative stress [1]. We have previously reported an important state of inflammation, where iNOS (inducible form of nitric oxide synthase) and COX-2 (cyclooxygenase-2) enzymes involved in NO (nitric oxide) metabolism play a significant role in lung injury as a result of zinc deficiency [2].

The pulmonary tissue stores labile zinc in a vesicle-like compartment. Labile zinc can be rapidly mobilized by stress state and may arise from zinc bound to metallothioneins (MTs) [3]. We also showed that zinc deficiency increases total MT levels during oxidative stress, probably due to a protective response to low zinc concentrations [2].

Received 22 November 2008; accepted 22 May 2009

Verónica S. Biaggio and Susana R. Valdéz are Fellows from the National Council of Scientific and Technical Investigations (CONICET).

María S. Gimenez is Career Scientific Investigator from CONICET.

Susana R. Valdéz is Scientific member of CONICET–Institute of Basic Sciences of National University of Cuyo, Mendoza, Argentina.

This research work was supported by a grant from CONICET (no. 4931) and National University of San Luis, Project No. 8104. The authors would like to thank Drs. A. Acosta, L. Gatica, S. Varas, J. Chediak, and S. Alvarez and Mr. R. Dominguez for their technical assistance.

Corresponding author: Dra. Nidia N. Gómez or Dra. María Sofía Giménez, Laboratorio de Bioquímica Molecular, Universidad Nacional de San Luis, Chacabuco y Pedernera, 5700, San Luis, Argentina.

E-mail: ngomez@unsl.edu.ar; mgimenez@unsl.edu.ar

The lungs have a potentially high risk of injury mediated by free radicals and lipid peroxidation [4]. Moreover, the lung tissue contains unsaturated fatty acids, which are a substrate for lipid peroxidation. Under certain stress conditions, the peroxidation of membrane lipids seems to be an unavoidable process in tissue injury [5].

This inflammatory process provokes the induction of high levels of a reactive oxygen species (ROS), which subjects the cell to a state of oxidative stress, and may damage cellular DNA, proteins, and lipids, and result in cell-cycle arrest, cellular senescence, and cell death [5]. ROS, such as superoxide, hydrogen peroxide ( $H_2O_2$ ), and hydroxyl radicals, are an inevitable consequence of mitochondrial respiration in aerobic organisms. Other sources of ROS generation are NADPH oxidases [6]; however, little is known about the relation between ROS production by NADPH oxidase and acute lung injury.

During the course of lung injury, various adhesive and proinflammatory molecules are generated, such as tumor necrosis factor alpha ( $TNF\alpha$ ) and vascular cell adhesion molecule (VCAM)-1 [7].  $TNF\alpha$  plays an important role during lung injury by activating nuclear factor kappa B ( $NF-\kappa B$ ), which increases gene transcription and synthesis of inflammatory proteins and growth factors [8]. This state causes neutrophils activation, which leads to expression of adhesion molecules in the surface of endothelial cells [9, 10] and induces a strong adherence between them. In previous research, we showed important polymorphonuclear neutrophils (PMNs) infiltration in zinc-deficient lung, and we also demonstrated the increased activity of antioxidant enzymes in lung tissue, which confirmed the oxidative stress and the local inflammation [2].

In addition, as a critical component of the cell's antioxidant defense system, zinc appears to be important for maintaining an environment that facilitates normal protein-protein interaction. Zinc deficiency can induce cell injury or inadequate tissue repair, which may have important implications in the pulmonary function. This might similarly be relevant for the optimal functioning of zinc-dependent proteins and transcriptions factors, such as peroxisome proliferator-activated receptor gamma ( $PPAR\gamma$ ) [11].

Moreover,  $PPAR\gamma$  has anti-inflammatory actions, and has been proved to down-regulate inflammatory response genes by negatively interfering with the nuclear factor  $NF-\kappa B$ , and regulating antioxidant enzymes activities, such as catalase [12]. Therefore, zinc deficiency has an important effect on the gene transcription of  $PPAR\gamma$  during lung injury. In spite of this, little is known about it, in the course of supplementation period.

The formation of reactive-nitrogen species (RNS) [13] and nitrosative stress are potentially involved in lung pathogenesis. According to this, both iNOS [2] and epithelial NOS (eNOS) expressions are related to an inflammatory process present in airways of acute lung injury. eNOS is expressed in human bronchial epithelium and in type II human alveolar cells, and it plays an important role during lung injury [13].

Recent data show that fibroproliferation and fibrosis can occur independently of inflammation, and that inflammation is required to initiate growth factors production. Mesenchymal growth factors—including transforming growth factor ( $TGF$ )- $\beta$  and insulin-like growth factor (IGF)-1, as well as proinflammatory cytokines, such as tumor necrosis factor alpha ( $TNF\alpha$ ) and interleukin-1 $\beta$ —have been shown to be exaggerated in several fibrotic lung disorders, including idiopathic pulmonary fibrosis (IPF), acute respiratory distress syndrome (ARDS), sarcoidosis, and bronchopulmonary dysplasia, as well as in pulmonary manifestations of systemic diseases [14]. Indirect mechanisms such as hormonal or metabolic alterations secondary to zinc depletion could contribute to impaired IGF-1 gene expression. The mechanisms by which zinc regulates IGF-I gene expression [15] and IGF-binding protein (IGFBP)-5 are not well known.

The present study was conducted to evaluate the relationship between zinc deficiency and IGF-1 and IGFBP-5 gene transcription in lung tissue, associated to changes in the gene transcription of NADPH oxidase, antioxidant enzymes, and zinc-dependent transcriptions factors. Moreover, we tried to analyze and to link the morphometrical changes to the parameters mentioned above. Finally, we also investigated the effect of restoring zinc levels to zinc-deficient rats on the different parameters associated with inflammation.

## MATERIALS AND METHODS

### Diet and Experimental Design

Male rats of the Wistar strain ( $200 \pm 10$  g) were used. Throughout the experiment, all rats were housed under controlled conditions ( $24^\circ C \pm 0.5^\circ C$  and 12 hours of light from 6 AM to 6 PM). Diet acclimation lasted 1 week. During that time, control diet (AIN 93-M) [16] was provided to all rats, and intake was measured. During the pretest, rats with similar intake profiles were matched and randomly assigned to the control or the Zn-deficient groups; each group contain 14 animals. Zn-adequate control diet (Co) contained 30 mg Zn/kg (as  $ZnCl_2$ ), and Zn-deficient diet (ZD) contained 5 mg Zn/kg. ZD animals were divided into 2 subgroups, and the last 10 days before sacrifice, one subgroup of deficient animals was fed

with the control diet (ZD-refed group), in order to supply these animals with ion zinc. The other subgroup, on the other hand, was fed with a ZD diet during the whole period of treatment. After 8 weeks of treatment, the animals were sacrificed. Fresh diets were given, and leftover food was discarded on a daily basis (20 g per day were enough to ensure “ad libitum” feeding). All the components of the diet remained constant (except for Zn contents), and were supplemented with recommended amounts of vitamins and minerals, according to an AIN 93-M diet [16]. Both diets had the following composition (g/kg): 466 cornstarch, 140 casein (785% protein), 155 dextrinized cornstarch, 100 sucrose, 50 fiber/cellulose, 40 soybean oil (containing liposoluble vitamins), 35 mineral mix AIN-93M-MX (zinc was not incorporated into the mineral mix of ZD diet), 10 vitamin mix (AIN-93-VX), 1.8 L-cystine, 0.008 ascorbic acid, 2.5 choline bitartrate (41% choline). All dietary ingredients were monitored for zinc concentration using atomic absorption spectrophotometry (AAS). Recommended guidelines [17] for rat care and treatment were followed. During the experience, body weights were registered weekly.

### Serum and Tissue Collection

At the end of the second month of treatment and 12 h after the last feeding, the animals were killed. Before that, they were anesthetized intraperitoneally (IP) with sodium pentobarbital (50 mg/kg), and blood samples for determination of zinc serum were collected in tubes previously washed and rinsed with nitric acid. The lungs were quickly removed, washed with ice-cold 0.9% saline solution, and weighed. Serum and right lobes of each lung were frozen at  $-80^{\circ}\text{C}$  until they were analyzed.

### Zinc Analysis

Aliquots of the diet, serum, and lung were collected without allowing any contact with metal. Each sample was wet-ashed with 16 N nitric acid, as described by Clegg et al. [18]. Zn concentrations of the pretreated samples and serum were quantified by an atomic absorption spectrophotometer (model 5100, HGA-600 Graphite Furnace; Perkin-Elmer). A linear calibration curve using certified standard National Institute of Standards and Technology (NIST) solutions was carried out. All specimens were diluted using bidistilled, deionized water, and analyzed in duplicate. Before sample digestion, different amounts of standard solution of each element were added. Recovery was between 98% and 99.2% for different elements.

### Thiobarbituric Acid-Reactive Substance (TBARS) Determination

Lung homogenates were used for TBA assay [19], and the levels of lipid peroxidation products, mainly malondialdehyde (MDA), were determined spectrophotometrically as TBARSs.

### RNA Isolation and Reverse Transcriptase-Polymerase Chain Reaction (RT-PCR) Analysis

A lobe was used by total RNA analyses. Total RNA was isolated by using TRIzol (Life Technologies). All RNA isolations were performed as instructed by the manufacturers. Gel electrophoresis and ethidium bromide staining confirmed the purity and integrity of the samples. Quantification of RNA was based on spectrophotometric analysis at 260/280 nm. Ten micrograms of total RNA were reverse-transcribed with 200 units of Moloney murine leukemia virus (MMLV) reverse transcriptase (Promega) using random hexamers as primers in a 20- $\mu\text{L}$  reaction mixture, following the manufacturers instructions. RT-generated fragments code for superoxide dismutase (SOD-2), glutathione peroxidase (GPx-1), catalase (CAT) and NAD(P)H oxidase (NOX-2) [20], tumor necrosis factor alpha (TNF $\alpha$ ) [21], metallothioneins I and II (MT I and II) [22], insulin growth factor-1 (IGF-1), insulin growth factor-binding protein-5 (IGFBP-5) [15], peroxisome proliferator-activated receptor gamma (PPAR $\gamma$ ) [23], vascular cell adhesion molecule-1 (VCAM-1) [24], and  $\beta$ -actin [25]. PCR was performed in 35  $\mu\text{L}$  of reaction solution containing 0.2 mM dNTPs, 1.5 mM MgCl<sub>2</sub>, 1.25 U of Taq polymerase, 50 pmol of each rat specific oligonucleotide primers, and RT products (1/10 of RT reaction). The expected PCR product of NOX-2 is 150 bp, SOD-2 is 191 bp, GPx-1 is 245 bp, CAT is 175 bp, TNF $\alpha$  is 400 pb, MT I is 312 pb, MT II is 297 pb, PPAR $\gamma$  is 131 pb, IGF-1 is 299 pb, IGF-BP5 is 399 pb, VCAM-1 is 476 pb, and  $\beta$ -actin is 243 bp. The samples were heated to 94 $^{\circ}\text{C}$  for 2 min, followed by 38 temperature cycles. Each cycle consisted of 3 periods: (1) denaturation, 94 $^{\circ}\text{C}$  for 1 min; (2) annealing, 60 $^{\circ}\text{C}$  for SOD-2, GPx-1, CAT, NOX-2, TNF $\alpha$ , PPAR $\gamma$ , and  $\beta$ -actin; 58 $^{\circ}\text{C}$  for IGF-1 and IGFBP-5; 65 $^{\circ}\text{C}$  for VCAM-1; 55 $^{\circ}\text{C}$  for MT I and II; for 1 min; (3) extension, 72 $^{\circ}\text{C}$  for 1 min. After 38 reaction cycles, the extension reaction continued for 5 more minutes. The PCR products were electrophoresed on 2% agarose gel with 0.01% ethidium bromide. The image was visualized and photographed under ultraviolet (UV) transillumination. The PCR was carried

out using primers specific to the following rat proteins:

NOX forward: 5' CCAGTGTGTCGGAATCTC-CCT 3'

reverse: 5' ATGTGCAATGGTGTGAATGG 3'

SOD-2 forward: 5' AGCTGCACCACAGCAAG-CAC 3'

reverse: 5' TCCACCACCCTTAGGGCTCA 3'

GPx-1 forward: 5' CGGTTTCCCGTG-CAATCAGT 3'

reverse: 5' ACACCGGGGACCAAATGATG 3'

CAT forward: 5' CGACCGAGGGATTCCAGATG 3'

reverse: 5' ATCGGGGTCTTCCTGTGCAA 3'

MT I forward: 5'ACTGCCTTCTTGTCGCTTA 3'

reverse: 5' TGGAGGTGTACGGCAAGACT 3'

MT II forward: 5' CCAACTGCCGCCTC-CATTCG 3'

reverse: 5' GAAAAAAGTGTGGAGAACCG 3'

TNF forward: 5' AAGTTCCCAAATGGCCTCC-CTCTCATC 3'

reverse: 5' GGAGGCTGACTTTCTCCTGGTAT-GAA 3'

PPAR forward: 5' TTCTGAAACCGACAGTACT-GACAT 3'

reverse: 5' CATGCTTGTGAAGGATGCAAG 3'

IGF-1 forward: 5' AAAATCAGCAGTCTTCCAAC 3'

reverse: 5' AGATCACAGCTCCGGAAGCA 3'

IGFBP-5 forward: 5' TTGCCTCAACGAAAA-GAGC 3'

reverse: 5' AGAATCCTTTGCGCGGTCACA 3'

VCAM-1 forward: 5' CACCTCCCCCAAGAAT-ACAGA 3'

reverse: 5' GCTCATCCTCAACACCCACAG 3'

Actin forward: 5' CGTGGGCCGC-CCAGGCACCA 3'

reverse: 5' TTGGCCTTAGGGTTCAGAGGG 3'

The intensity of each band was measured using the NIH Image software and reported as the values of band intensity units. The relative abundance of each target band was then normalized according to the housekeeping gene  $\beta$ -actin, calculated as the ratio of the intensity values of each target product to that of  $\beta$ -actin.

### Western Blot Analysis for eNOS

Lungs were homogenized with 50 mM Tris-HCl (pH 7.8) containing 0.01% Triton X100 and protease inhibitor cocktail, and centrifuged at 4°C. Protein concentrations of the resulting supernatants were determined according to the method of Wang and Smith

[26], using bovine serum albumin (BSA) as a standard. Forty micrograms of proteins were mixed with 10  $\mu$ L of sample buffer (125mM Tris-HCl, pH 6.8, 4% sodium dodecyl sulfate [SDS], 3.5 mM dithiothreitol [DTT], 0.02% bromophenol blue, and 20% glycerol), boiled for 2 to 3 minutes, and loaded into a 10% SDS-polyacrylamide gel electrophoresis (PAGE) gel. Protein molecular mass markers were always loaded on each gel. Separated proteins were transferred to polyvinylidene difluoride (PVDF) membranes (Polyscreen NEF 1000; NEN Life Science Products) using a blot transfer system (BioRad Laboratories, Hercules, CA). After being blocked with 5% BSA-TBS solution (20 mM Tris, 500 mM NaCl, pH 7.5) overnight, at 4°C with gentle agitation, membranes were incubated with a primary rabbit anti-eNOS polyclonal antibody (1:1000 dilution) for 1 hour (Santa Cruz Biotechnology). After washing 3 times with TTBS (0.1% Tween 20, 100 mM Tris-HCl, pH 7.5, 150 mM NaCl), membranes were incubated with a secondary goat anti-rabbit immunoglobulin G (IgG) antibody linked to biotin for 1 h at room temperature (1:2000 dilution). Membranes were washed again and the color was developed using a Vectastain ABC detection system (Vector Labs). The intensity of the bands was scanned densitometrically with the image processing and analysis programme Scion Image and expressed on arbitrary units.

### Histological and Morphometric Examination of Lung

The lungs from 6 rats in each group and at each time point were fixed in situ for microscopy by intratracheal instillation of Bouin's solution at 20 cm H<sub>2</sub>O pressure for 10 minutes, subsequently removed from the thorax, and immersed in a fixative for 2 hours [2]. The samples were dehydrated in graded series of ethanol and embedded in paraffin. Sections of 5 to 6  $\mu$ m thickness were obtained using a Porter Blum Hn40 microtome and stained with hematoxylin and eosin (H&E). Histological observations were made on at least 4 sections of the different regions of each lung lobe. Microphotographs were taken using an Olympus BX50 microscope connected to a digital camera and to a PC-based image analysis system (Image J) [27]. Sections were examined for evidence of lung injury by light microscopy, which were scored for edema and neutrophil infiltration. A 5-point scale (0 to 4) was used to represent severity: 0 for no or very minor severity, 1 for modest and limited, 2 for intermediate, 3 for widespread or prominent, and 4 for widespread and most prominent [28].

## Statistical Analysis

For each set of values, the mean and standard error of the mean were calculated and compared using 1-way analysis of variance (ANOVA) [29], with the statistical computer analysis system GraphPad Prism. When ANOVA revealed statistical differences, the statistical post hoc analysis of Bonferroni was used. When the assays were of 2 groups, the statistical differences were tested by Student's test. Fisher least significance difference test was used to examine differences between group means. Significance was set at the  $P < .05$  level.

## RESULTS

### Weight Gain and Zn Status of the Rats

Table 1 shows the body weight of rats fed with a ZD diet, which was significantly lower than the control one after 2 months of treatment, whereas the weight of the ZD-refed group was significantly higher compared to the ZD group. Zinc concentrations in serum and lung decreased in the ZD group, whereas the level of zinc in the ZD-refed group surpassed the control values. In our experimental model, clinical signs such as dermatitis or alopecia were not observed.

### Expression of Metallothioneins I and II

Another parameter used to confirm zinc deficiency in our model was the determination of gene

TABLE 1 Body and Lung Weights, Zinc Concentrations, and TBARS of Male Rat

	Co	ZD	ZD refed
Body weight (g)	384 ± 10.7	323 ± 6.7**	391 ± 15.3
Zn in lung (ppm)	2.46 ± 0.75	1.13 ± 0.40**	1.66 ± 0.28
Zn in serum ( $\mu\text{mol/L}$ )	7.6 ± 1.5	2.4 ± 0.7**	8.2 ± 2.5
TBARS (nM/mg prot)	2.89 ± 0.59	10.9 ± 1.5***	13.8 ± 0.7***

Note. Results given as means ± SEM,  $n = 14$  for each case. Across a row, values with different superscript indicate differences by ANOVA test.

Mean values were significantly different (\*\* $P < .01$ , \*\*\* $P < .001$ ) when compared to control group.

transcription of metallothioneins I and II, mainly MT II (Figure 1). It is well established that MT II plays an important role in the zinc metabolism. MT II mRNA transcription increased in the ZD group as compared to the control group, but during the supplementation period, MT II gene transcription was decreased compared to the control. The gene transcription of MT I was not significantly different among all groups.

### Thiobarbituric Acid-Reactive Substances

TBARSs were measured by levels of MDA in lung tissue. Table 1 summarizes the effect of ROS and RNS production on the lipid metabolism and shows an enhanced lipid peroxidation in the ZD group

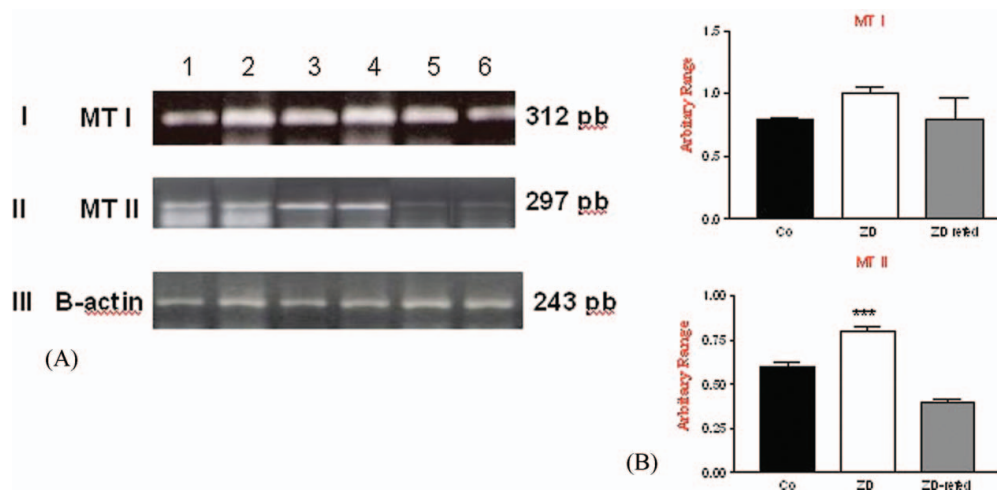


FIGURE 1 (A) Transcription of metallothionein I and II in control and ZD rats. I: Ethidium bromide-stained agarose gel of MT I PCR products. II: Ethidium bromide-stained agarose gel of MT II PCR products. Ethidium bromide-stained agarose gel of  $\beta$ -actin PCR products, used as an internal control. Lanes 1, 2: control samples. Lanes 3, 4: ZD samples. (B) Quantification of the intensity of the fragment bands in relation to the intensity of the internal control bands ( $n = 8$  per dietary group). \*\*\* $P < .001$  significance when compared to controls.

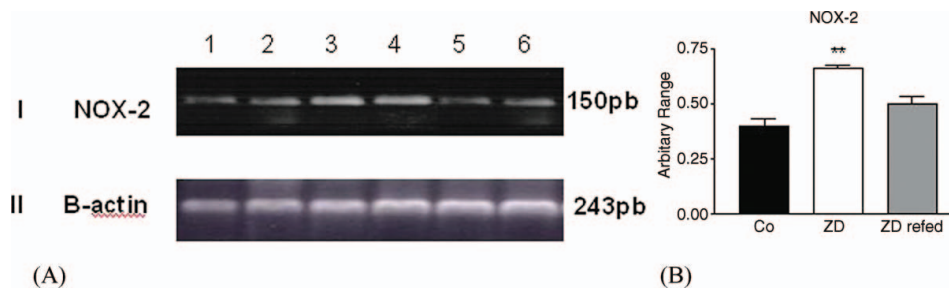


FIGURE 2 (A) Transcription of NADPH oxidase (NOX-2) in control, ZD, and ZD-refed group. I: Ethidium bromide-stained agarose gel of NOX-2 PCR products. II: Ethidium bromide-stained agarose gel of  $\beta$ -actin PCR products, used as an internal control. Lanes 1, 2: control samples. Lanes 3, 4: ZD samples. Lanes 5, 6: ZD-refed samples. (B) Quantification of the intensity of the fragment bands in relation to the intensity of the internal control bands ( $n = 8$  cases per group). \*\* $P < .05$  significance when compared to controls.

( $P < .001$ ). Total lung MDA levels in the ZD-refed group were significantly higher than the control.

### Expression of NADPH Oxidase (NOX-2)

One of the most important sources of superoxide is NADPH oxidase. There are several isoforms of NADPH oxidase, one of which is NOX-2. Given the fact that local inflammation produces an increase of superoxide level, we determined NOX-2 mRNA transcription in lung, which was significantly higher in the ZD group (Figure 2). Gene transcription of NOX-2 in the ZD-refed group decreased to control values.

### Expression of Superoxide Dismutase (SOD-2), Glutathione Peroxidase (GPx-1), and Catalase (CAT)

As a consequence of oxidative damage, the antioxidant mechanism induces the gene transcription of enzymes of the antioxidant system. For this reason, we measured SOD-2, GPx-1, and CAT mRNA transcription during lung injury. The gene transcription of SOD-2 was significantly higher in the ZD group; therefore, the concentration of  $H_2O_2$  increased. However, after a short refeeding time, SOD-2 transcription decreased in the ZD-refed group.  $H_2O_2$  is further decomposed to  $H_2O$  by action of GPx-1 and CAT. GPx-1 mRNA transcription was significantly higher in the ZD and refed groups. In contrast, CAT mRNA transcription did not change among all the groups (Figure 3).

### Expression of Tumor Necrosis Factor Alpha (TNF $\alpha$ )

The levels of TNF $\alpha$  were measured after exposure to zinc deficiency by RT-PCR analysis. Gene transcrip-

tion of TNF $\alpha$  was significantly increased in the ZD group ( $P < .05$ ), whereas this response was significantly higher in the ZD-refed group ( $P < .005$ ) than the control (Figure 4).

### Expression of Vascular Cell Adhesion Molecule (VCAM-1)

To further characterize the mechanism that underlies high neutrophil influx in the lung in response to zinc deprivation, VCAM-1 mRNA transcription was determined by RT-PCR analysis. VCAM-1 mRNA transcription increased in the ZD group when compared to the control. In contrast, in the ZD-refed group, the gene transcription of VCAM-1 decreased compared to control group (Figure 5).

### Expression of Peroxisome Proliferator-Activated Receptor Gamma (PPAR $\gamma$ )

The effect of zinc deficiency and supplementation in the gene transcription of PPAR- $\gamma$  was studied (Figure 6). This transcription factor contains "zinc fingers" in its structure. PPAR- $\gamma$  mRNA transcription was markedly reduced during zinc deficiency, and the time of refeeding was not sufficient to recover the gene transcription (ZD refed).

### Expression of Endothelial Nitric Oxide Synthase (eNOS)

We determined the expression of eNOS by Western blot techniques. The results showed an increase of eNOS expression in the ZD group when compared to the control group. The expression in ZD-refed group of eNOS did not overtake the level of control group (Figure 7).

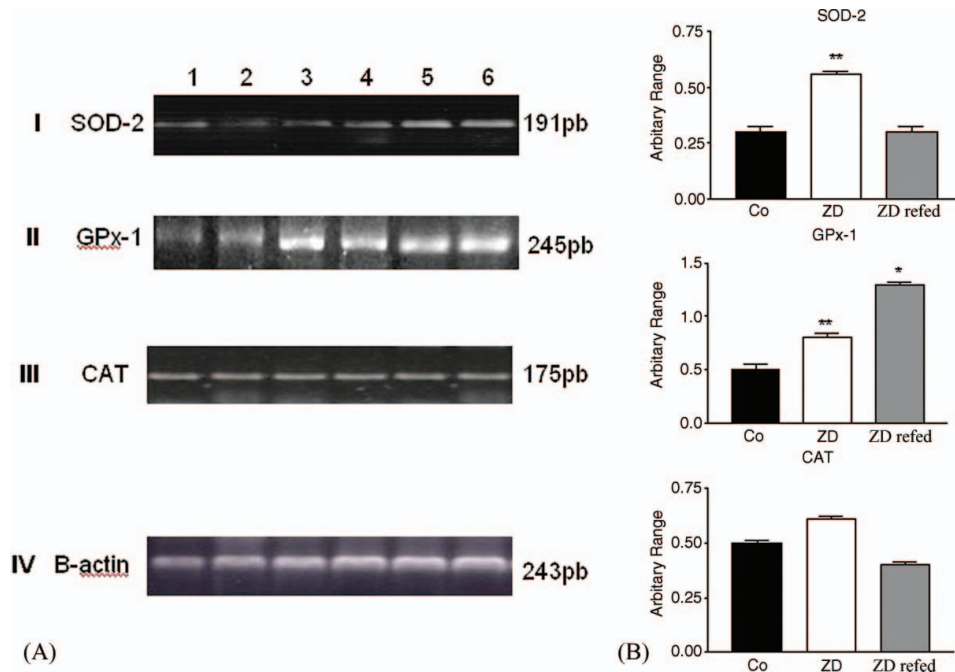


FIGURE 3 (A) Transcription of enzymes of the antioxidant system in control, ZD, and ZD-refed rats. I: Ethidium bromide-stained agarose gel of SOD-2 PCR products. II: Ethidium bromide-stained agarose gel of GPx-1 PCR products. III: Ethidium bromide-stained agarose gel of CAT PCR products. IV: Ethidium bromide-stained agarose gel of  $\beta$ -actin PCR products, used as an internal control. Lanes 1, 2: control samples. Lanes 3, 4: ZD samples. Lanes 5, 6: ZD-refed samples. (B) quantification of the intensity of the fragment bands in relation to the intensity of the internal control bands ( $n = 8$  cases per group). \* $P < .01$ , \*\* $P < .05$  significantly different than controls.

### Lung Histopathology

The lungs were fixed, sectioned, stained, and examined for evidence of lung injury. Significant morphological changes in lung parenchyma were observed in ZD rats when compared to the control group after 2 months of treatment (Figure 8). A section of ZD shows accumulation of abundant polymorphonuclear infiltration in the lung, with thickened

alveolar septae, alternated collapsed and expanded alveoli, inflammation, and edema. Similarly, ZD lung exhibited hypertrophy due to an increase of connective tissue fibers. A section of the ZD-refed group shows polymorphonuclear infiltration, severe inflammation, expanded alveoli, and focal interstitial proliferation. The significant changes observed in the histological appearance in lung of ZD and ZD-refed group reflect their susceptibility to injury.

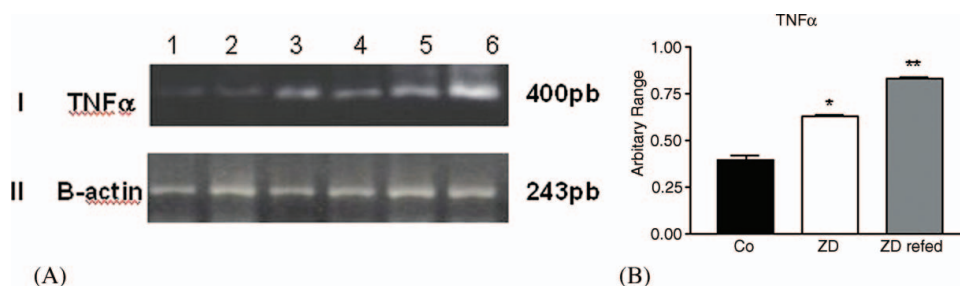


FIGURE 4 (A) Transcription of tumor necrosis factor (TNF $\alpha$ ) in control, ZD, and ZD-refed rats. I: Ethidium bromide-stained agarose gel of TNF $\alpha$  PCR products. II: Ethidium bromide-stained agarose gel of  $\beta$ -actin PCR products, used as an internal control. Lanes 1, 2: control samples. Lanes 3, 4: ZD samples. Lanes 5, 6: ZD-refed. (B) Quantification of the intensity of the fragment bands in relation to the intensity of the internal control bands ( $n = 8$  per dietary group). \* $P < .05$ , \*\* $P < .005$  significantly different than controls.

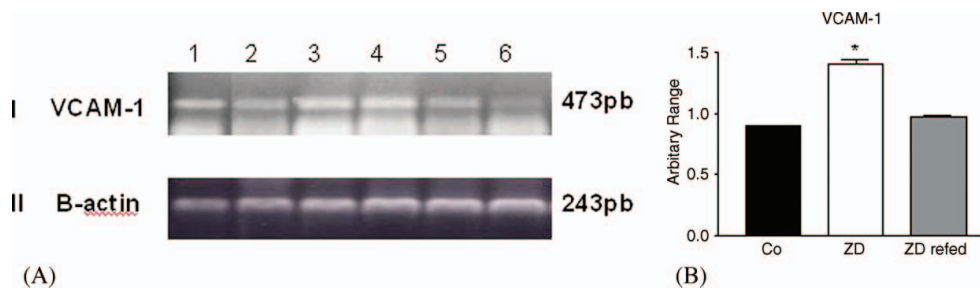


FIGURE 5 (A) Transcription of vascular cell adhesion molecule (VCAM-1) in control, ZD, and ZD-refed rats. I: Ethidium bromide-stained agarose gel of VCAM-1 PCR products. II: Ethidium bromide-stained agarose gel of  $\beta$ -actin PCR products, used as an internal control. Lanes 1, 2: control samples. Lanes 3, 4: ZD samples. Lanes 5, 6: ZD-refed samples. (B) Quantification of the intensity of the fragment bands in relation to the intensity of the internal control bands ( $n = 8$  per dietary group). \* $P < .01$  significance when compared to controls.

### Expression of Insulin Growth Factor-1 (IGF-1) and Insulin Growth Factor-Binding Protein (IGFBP-5)

We examined the influence of zinc deprivation in the gene transcription of some growth factors, such as IGF-1 and IGFBP-5. As shown in Figure 9, gene transcription of IGF-1 decreased whereas gene transcription of IGFBP-5 increased ( $P < .05$ ) in the ZD group. The gene transcription of IGF-1 ( $P < .001$ ) and IGFBP-5 ( $P < .01$ ) in the ZD-refed group were higher than control group.

### DISCUSSION

Mild-to-moderate zinc deficiency is frequently reported in developing countries. However, the prevalence of mild deficiency in industrialized countries is unknown due to the lack of sensitive clinical biomarkers of zinc status.

Previous works have shown a clear association between lung and oxidative stress. Also, a number of in vitro and in vivo studies have shown increased oxidative stress, specifically in the airways [30, 31] following zinc deprivation, but few works related the lung parenchyma to this situation [32–34]. We demonstrated that NO-related species are accumulated in the lung during the course of zinc deficiency [2]. Under pathological conditions, this situation is interesting because NO and superoxide anion are produced at high levels, and can react extremely fast in order to form the potent oxidant peroxynitrite [2]. Considering this, we examined ZD animals in search of changes in the gene transcription of antioxidant enzymes, and proinflammatory factors, among others, in lung stromal. We refed those animals with a control diet for 10 days in order to determine if there was recovery of some of the parameters. We also studied what happened with some factors such as IGF-1 and its regulator IGFBP-5. We used an experimental model that has the advantage of having been used for

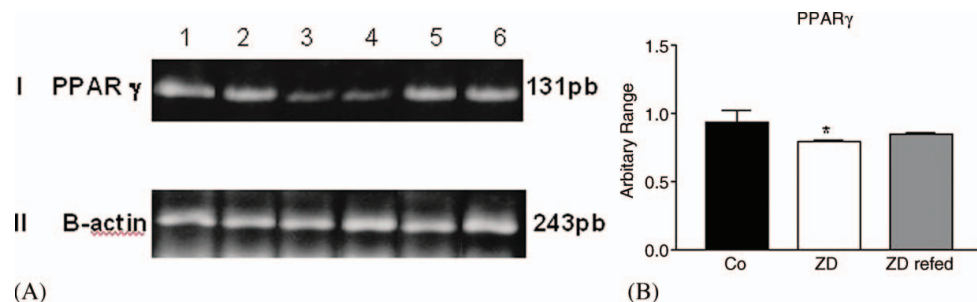


FIGURE 6 (A) Transcription of peroxisome proliferator-activated receptor gamma (PPAR $\gamma$ ) in control, ZD, and ZD-refed rats. I: Ethidium bromide-stained agarose gel of PPAR $\gamma$  PCR products. II: Ethidium bromide-stained agarose gel of  $\beta$ -actin PCR products, used as an internal control. Lanes 1, 2: control samples. Lanes 3, 4: ZD samples. Lanes 5, 6: ZD-refed samples. (B) Quantification of the intensity of the fragment bands in relation to the intensity of the internal control bands ( $n = 8$  per dietary group). \* $P < .01$  significance when compared to controls.



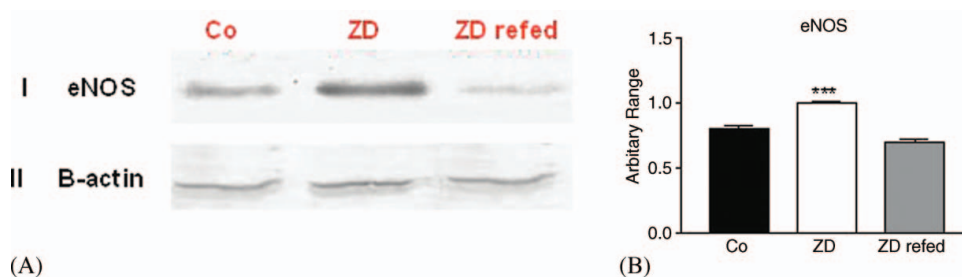


FIGURE 7 (A) Immunoblot analysis of endothelial NO synthase (eNOS) expression in lung. Representative experiment of Western blot is shown. I: eNOS expression was detected with an anti-eNOS antibody. II:  $\beta$ -actin was used as an internal control. (B) Quantification of the protein band corresponding to eNOS was performed by densitometry. Results show intensity of eNOS band in relation to the intensity of the internal control band ( $n = 8$  per dietary group). \*\*\* $P < .001$  significance when compared to controls.

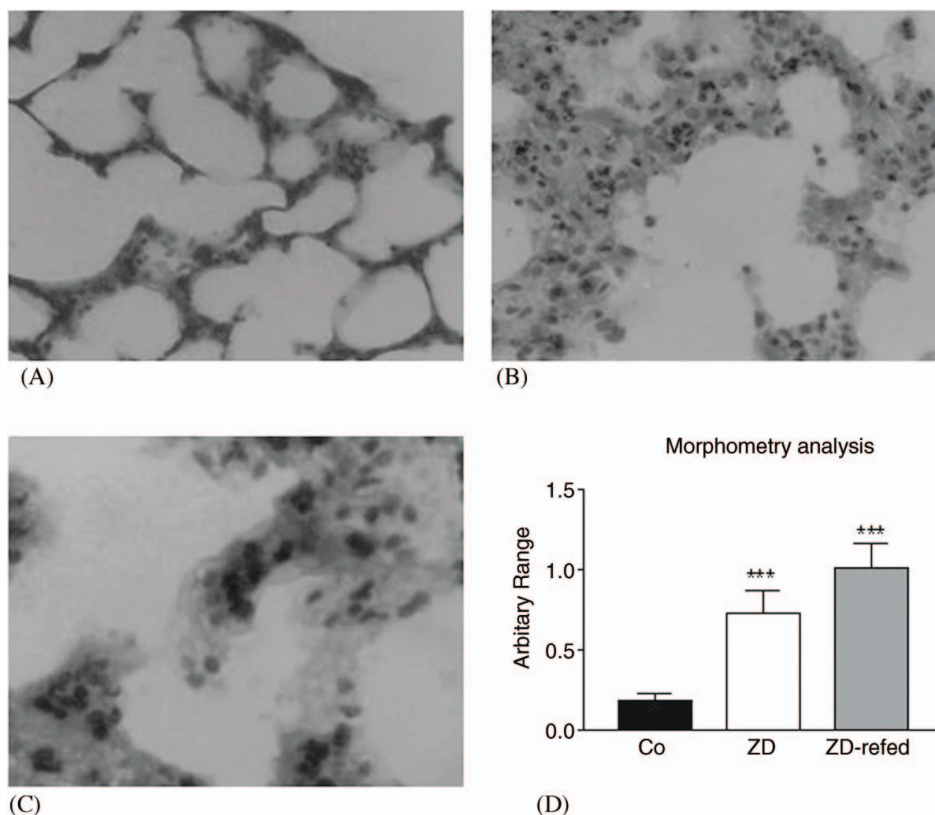


FIGURE 8 Histological assessment of the effect of zinc deficiency (ZD), and zinc refeeding (ZD refed) in lung. The lungs from 6 rats in each group and at each time point were fixed in situ by intratracheal instillation of Bouin's solution at 20 cm  $H_2O$  pressure for 10 minutes, and immersed in addition fixative. The samples were dehydrated in graded series of ethanol and embedded in paraffin. Sections were stained with hematoxylin-eosin ( $300\times$ ). (A) Control (Co) lungs show preserved lung parenchyma architecture. (B) ZD show prominent polymorphonuclear infiltration, thickened alveolar septae, inflammation, edema, and hypertrophy of connective tissue. (C) These features were not diminished in rat treated with control diet. ZD refed show clear cells infiltration, over expanded alveoli, inflammation, edema, and focal interstitial proliferation. (D) Morphometric examination of the lungs. Each bar represents the mean  $\pm$  SEM of alveolar space in each group. \*\*\* $P < .001$  significantly different than Co.

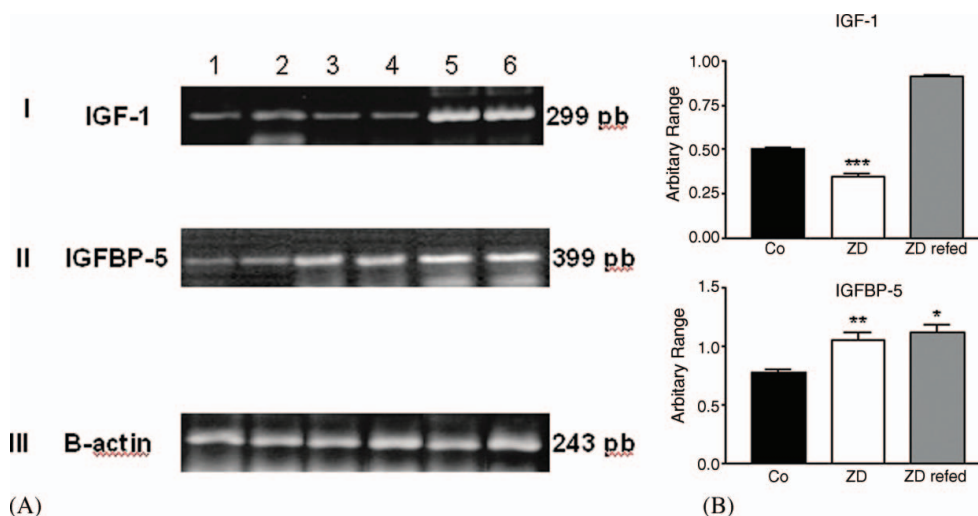


FIGURE 9 (A) Transcription of insulin growth factor (IGF-1) and Insulin growth factor-binding protein (IGFBP-5) in control, ZD, and ZD-refed rats. I: Ethidium bromide-stained agarose gel of IGF-1 PCR products. II: Ethidium bromide-stained agarose gel of IGFBP-5 PCR products. III: Ethidium bromide-stained agarose gel of  $\beta$ -actin PCR products, used as an internal control. Lanes 1, 2: control samples. Lanes 3, 4: ZD samples. Lanes 5, 6: ZD-refed samples. (B) Quantification of the intensity of the fragment bands in relation to the intensity of the internal control bands ( $n = 8$  per dietary group). \* $P < .01$ , \*\* $P < .05$ , \*\*\* $P < 0.001$  significantly different than control.

a long time to obtain more relevant physiological results [33–35]. In our experimental design, Zn deprivation for 8 weeks induces decrease of body weight in the ZD group and Zn refeeding restores the body weight in the ZD refed group (Table 1), and confirms previous results [2, 33].

A decrease in serum zinc increased the risk for developing metabolic and clinical signs of zinc deficiency [36] and confirmed previous data [2, 34]. During the supplementation period, serum zinc concentration increased in relation to ZD. Some authors have shown that when zinc is added back to the diet, growth is promptly resumed, and it initially proceeds even faster than in the controls [37]; the time of refeeding used in this work was enough to overtake the normal level of zinc.

In addition, zinc homeostasis is regulated by MTs, which control the uptake, distribution, storage, and release of zinc during oxidative damage [38, 39], and MTs appear to act as a component of cellular defenses [40, 41]. Also, MTs could play an important role in the intracellular signal transduction pathways [38, 39, 42]. We think that the increased gene transcription of MT II in our experimental model is associated to zinc deficiency [33]. MT I transcription did not change in either group (Figure 1).

In an inflammatory environment, ROS production is activated, and ROS can attack not only DNA, but also other cellular components such as polyunsaturated fatty acid residues of phospholipids, which are

extremely sensitive to oxidation [43]. In our model, the increase of TBARS levels might be attributed to high concentrations of hydroperoxides arising from polyunsaturated fatty acid, among others [44]. However, in the ZD-refed group, TBARS levels did not decrease to the level of control group (Table 1). Apparently, such a brief refeeding period of time is not enough to overcome the redox changes induced by the zinc deficiency.

It is known that part of ROS production is normally generated by tightly regulated enzyme NAD(P)H oxidase isoforms, which are best characterized in neutrophils, and contribute to a large number of pathologies, in particular chronic inflammation [45, 46]. Activated PMNs generate extracellular superoxide anions through a plasma membrane NADPH oxidase, which is expressed at high levels in these cells [45, 46]. Inappropriate gene transcription or activation of NOX during various pathologies suggests their specific involvement in the disease. In addition, this is one of the first communications that relates the changes of NOX-2 to ZD. Our results demonstrated that NOX-2 transcription is increased in the ZD group; so the superoxide production could explain, at least in part, chronic inflammation in our experimental model. At the end of the supplementation period, the level of NOX-2 decreases in relation to ZD, which suggests that the superoxide concentration may be decreasing and the situation improves (Figure 2).

The mammalian cells present a specific antioxidant defense system that plays an important role during the inflammatory process. This system is formed by several enzymes, such as SOD, GPx, and CAT. In agreement with other authors [20, 47], we previously showed increased activity of enzymes of the antioxidant system in lung tissue of ZD rats [33]. We demonstrated that the gene transcription of SOD-2 in the ZD group increased, and that SOD-2 transcription in the ZD-refed group overtakes the control level. In fact, increased SOD-2 levels could decrease toxicity by decreasing superoxide availability and, therefore, lessen direct and indirect reactions of ROS with cellular constituents [47–49]. The H<sub>2</sub>O<sub>2</sub> content is further decomposed to water by CAT or GPx and considerable evidence suggests that GPx gene transcription increases in lung injury [48–50]. In the present study, the gene transcription of lung GPx-1 was higher in the ZD and ZD-refed groups when compared to the control group, and CAT transcription did not change in any of the groups (Figure 3); these results agree with the activities of this antioxidant enzyme [33].

The acute inflammatory response, as a consequence of zinc deprivation, produces several effects; one of them is the neutrophils activation [50]. The migration of neutrophils is mediated by the abnormal expression of adhesion molecules, which promotes a much firmer interaction with endothelial cells, probably by the abnormal induction of redox-sensitive signaling pathways [51]. Adhesion molecules, such as VCAM-1, may play a major role in recruitment PMNs and their subsequent retention in the airways [52]. Besides, the expression of adhesion molecules can be up-regulated by a number of cytokines, such as TNF $\alpha$  by activating NF- $\kappa$ B pathways [51], as shown in our previous results [2]. There is considerable evidence that pathophysiological concentrations of TNF $\alpha$  contribute to increased expression of VCAM-1 [53]. In addition, we demonstrated an increased transcription of TNF $\alpha$  and VCAM-1 in the ZD group (Figures 4, 5). Moreover, as we expected, the gene transcription of VCAM-1 decreased in the ZD-refed group, which suggests that the period of supplementation was enough to restore their control levels (Figures 4, 5).

On the other hand, it is well established that PPAR $\gamma$  interferes negatively with the nuclear factors NF- $\kappa$ B and TNF- $\alpha$ , which have also been identified as therapeutic targets in inflammation [54]. TNF- $\alpha$  is an important stimulus for the release of inflammatory mediators by airway smooth muscle cells and down-regulates the expression of inflammatory genes. In our experimental work, we demonstrated the decreased gene transcription of PPAR $\gamma$  in ZD

rats (Figure 6); but after 10 days of refeeding, its gene transcription increased even though it did not overtake the control level. This situation is associated to the higher increase of TNF $\alpha$  gene transcription in ZD-refed group, probably as a consequence, at least in part, of PPAR $\gamma$ .

eNOS is constitutively expressed in bronchial epithelium in type II alveolar epithelial cells and in pulmonary blood vessels [55]. We measured the expression of eNOS, which increased in the ZD group as compared to control, whereas in the ZD-refed group the level of eNOS did not overtake the level of control (Figure 7). In addition, recent studies have indicated that treatment of endothelial cells with H<sub>2</sub>O<sub>2</sub> can result in short-term increased eNOS activity [56], and chronic enhanced eNOS expression [57, 58]. Previously we measured the concentration of H<sub>2</sub>O<sub>2</sub> (data not shown) in the same model and we found that eNOS expression increased in parallel, which suggests a possible role of this enzyme during lung injury.

Under these conditions, the interaction among activated macrophages, infiltrated neutrophils, alveolar cells, and vascular endothelial cells in alveolar space potentiate moderate to severe inflammation, amplifying a cascade of inflammatory reactions and modification of the surfactant synthesis [59], and causing surfactant dysfunction [60, 61]. Moreover, histological studies showed an inflammatory situation with mononuclear inflammatory cells infiltration, edema, expanded alveoli, and interstitial proliferation in the ZD group. In the ZD-refed group, more significant changes in lung parenchyma were observed. The ZD-refed group revealed fragmentation of the alveolar septa, focal interstitial proliferation, edema, and mononuclear inflammatory cell infiltration (Figure 8). The significant changes observed in lung of the ZD and ZD-refed groups reflect their susceptibility to injury. This fact could be considered as a result of cellular oxidative and nitrosative damage.

An increasing number of reports indicate that changes in the oxidants levels are able to regulate the growth factor and cytokines-mediated signaling [62]. In addition, Krein et al. recognized the potential role of several growth factors in the fibroproliferative process in the lung, and they focused on the possible roles of the growth factors IGF-1 and TGF- $\beta$  in cell migration and proliferation [62]. PMN migration and proliferation and increased TGF- $\beta$  (data not show) were observed in our experimental model. In addition, IGF-1 has been shown to be elevated in the lungs of patients with IPF, fibroproliferative ARDS, and other fibrotic lung disorders, as well as in animal models of pulmonary fibrosis such as bleomycin-induced fibrosis [63].

In our results, IGF-1 gene transcription in ZD lung is decreased compared to control. Laboratory studies have shown that bone marrow-derived macrophages in the presence of TGF- $\beta$  has reduced basal IGF-1 mRNA production and, when stimulated with TNF $\alpha$ , macrophages have been unable to enhance IGF-1 messenger RNA production. Interestingly, other authors showed large numbers of IGF-1-immunoreactive cells in the early stages of IPF, whereas in later phases of the disease the presence of IGF-1-positive cells was significantly reduced. This situation is supported by the theory that IGF-1 acts early following inflammation to promote cell proliferation and that in later phases of the disease, when TGF- $\beta$  is present, IGF-1 has been negatively regulated.

Some researchers have previously demonstrated that IGFBP-5 increases in lung tissues of patients with lung fibrosis [14]. We demonstrated that IGFBP-5 transcription is increased in the ZD group compared to the control (Figure 9), which is also consistent with the morphological changes observed in the ZD group. During refeeding time, both IGF-1 and IGFBP-5 increases overtake the control values. The mechanisms by which zinc regulates IGF-1 gene expression have not been extensively studied. Alternatively, indirect mechanisms such as hormonal or metabolic alterations secondary to zinc depletion could also contribute to the impaired IGF-1 gene transcription [64].

In conclusion, the present results suggest that moderate Zn deficiency produces alterations in the gene transcription of various antioxidant enzymes, proinflammatory genes, and growth factors such as IGF-1 in lung, which leads to histoarchitectural alterations. It would be important to apply the knowledge of Zn deficiency and its effects on lung in order to design public health interventions to address micronutrient malnutrition. When this situation occurs together with other pathologies in lungs, it could lead to worse prognosis in patients at risk.

**Declaration of interest:** The authors report no conflicts of interest. The authors alone are responsible for the content and writing of the paper.

## REFERENCES

[1] Zalewski P: Zinc metabolism in the airway: basic mechanisms and drug targets. *Curr Opin Pharmacol.* 2006;6:237–243.  
 [2] Gomez NN, Davicino RC, Biaggio VS, Bianco GA, Alvarez SM, Fischer P, Masnatta L, Ravinovich GA, Gimenez MS: Overexpression of inducible nitric oxide synthase and cyclooxygenase-2 in rat zinc-deficient lung: involvement of a NF- $\kappa$ B dependent pathway. *Nitric Oxide.* 2006;14:30–38.

[3] Berendji D, Kolb-Bachofen V, Meyer KL, Grapenthin O, Weber H, Wahn V, Kroncke KD: Nitric oxide mediates intracytoplasmic and intranuclear zinc release. *FEBS Lett.* 1997;405:37–41.  
 [4] Kovacheva S, Ribarov SR: Lipid peroxidation in lung of rats stressed by immobilization: effects of vitamin E supplementation. *Lung.* 1995;173:255–263.  
 [5] Liu J, Mori A: Stress, aging and brain oxidative damage. *Neurochem Res.* 1999;24:1479–1497.  
 [6] Lambeth JD: Nox enzymes, ROS, and chronic disease: an example of antagonistic pleiotropy. *Free Radic Biol Med.* 2007;43:332–347.  
 [7] Atsuta J, Sterbinsky SA, Plitt J, Schwiebert LM, Bochner BS, Schleimer RP: Phenotyping and cytokine regulation of the BEAS-2B human bronchial epithelial cell: demonstration of inducible expression of the adhesion molecules VCAM-1 and ICAM-1. *Am J Respir Cell Mol Biol.* 1997;17:571–582.  
 [8] Barnes PJ: Transcription factors in airway diseases. *Lab Invest.* 2006;86:867–872.  
 [9] Osborn L, Hession C, Tizard R, Vassallo C, Luhowskyj S, Chiorosso G, Lobb R: Direct expression cloning of vascular cell adhesion molecule 1, a cytokine-induced endothelial protein that binds to lymphocytes. *Cell.* 1989;59:1203–1211.  
 [10] Pohlman TH, Stanness KA, Beatty PG, Ochs HD, Harlan JM: An endothelial cell surface factor (s) induced in vitro by lipopolysaccharide, interleukin-1, and tumor necrosis factor- $\alpha$  increases neutrophil adherence by a CDw-18-dependent mechanism. *J Immunol.* 1986;136:4548–4553.  
 [11] Ricote M, Li AC, Wilson TM, Kelly CJ, Glass CK: The peroxisome proliferator-activated receptor- $\gamma$  is a negative regulator of macrophage activation. *Nature.* 1998;391:79–82.  
 [12] Girnun GD, Domann FE, Moore SA, Robbins ME: Identification of a functional peroxisome proliferator-activated receptor response element in the rat catalase promoter. *Mol Endocrinol.* 2002;16:2793–2801.  
 [13] Shaul PW, North AJ, Wu LC, Wells LB, Brannon TS, Lau KS, Mitchel T, Margraf LR, Star RA: Endothelial nitric oxide synthase is expressed in cultured human bronchiolar epithelium. *J Clin Invest.* 1994;94:2231–2236.  
 [14] Ninh NX, Maiter D, Verniers J, Lause P, Ketelslegers JM, Thissen JP: Failure of exogenous IGF-1 to restore normal growth in rats submitted to dietary zinc deprivation. *J Endocrinol.* 1998;159:211–217.  
 [15] Rosato R, Lindenbergh-Kortleve D, Neck J, Drop S, Jahn G: Effect of chronic thyroxine treatment on IGF-I, IGF-II and IGF-binding protein expression in mammary gland and liver during pregnancy and early lactation in rats. *Eur J Endocrinol.* 2002;146:729–739.  
 [16] Reeves PG, Nielsen FH, Fahey GC Jr: AIN-93 purified diets for laboratory rodents: final report of the American Institute of Nutrition ad hoc writing committee on the reformulation of the AIN-76A rodent diet. *J Nutr.* 1993;123:1939–1951.  
 [17] US Public Health Service: Guide to the Care and Use of Laboratory Animals. Bethesda, MD: National Institutes of Health; 1985:85–123.  
 [18] Clegg MS, Keen CL, Lonnerdal B, Hurley LS: Influence of ashing techniques on the analysis of trace elements in animal tissue. I. Wet ashing. *Biol Trace Elem Res.* 1981;3:107–115.  
 [19] Buege JA, Aust SD: Microsomal lipid peroxidation. *Methods Enzymol.* 1978;52:302–319.  
 [20] Tam NN, Gao Y, Leung YK, Ho SM: Androgenic regulation of oxidative stress in the rat prostate. Involvement of NAD(P)H oxidases and antioxidant defense machinery during prostatic involution and regrowth. *Am J Pathol.* 2003;163:2513–2522.  
 [21] Choi HC, Lee KY: CD14 glycoprotein expressed in vascular smooth muscle cells. *J Pharmacol Sci.* 2004;95:65–70.

- [22] Zeng X, Jin T, Zhou Y, Nordberg GF: Changes of serum sex hormone levels and MT mRNA expression in rats orally exposed to cadmium. *Toxicology*. 2003;186:109–118.
- [23] Hoekstra M, Kruijt JK, Van Eck M, Van Berkel TJ: Specific gene expression of ATP-binding cassette transporters and nuclear hormone receptors in rat liver parenchyma, endothelial, and Kupffer cells. *J Biol Chem*. 2003;278:25448–25453.
- [24] Pueyo ME, Gonzalez W, Nicoletti A, Savoie F, Arnal JF, Michel JB: Angiotensin II stimulates endothelial vascular cell adhesion molecule-1 via nuclear factor-kappaB activation induced by intracellular oxidative stress. *Arterioscler Thromb Vasc Biol*. 2000;20:645–651.
- [25] Choi JW, Choi HS: The regulatory effects of thyroid hormone on the activity of 3-hydroxy-3-methylglutaryl coenzyme A reductase. *Endocr Res*. 2000;26:1–21.
- [26] Wang C, Smith RL: Lowry determination of protein in the presence of Triton X-100. *Anal Biochem*. 1975;63:414–417.
- [27] Abramoff MD, Magelhaes PJ, Ram SJ: Image Processing with Image J. *Biophotonics Int*. 2004;11:36–42.
- [28] Zhou ZH, Sun B, Lin K, Zhu LW: Prevention of rabbit acute lung injury by surfactant, inhaled nitric oxide, and pressure support ventilation. *Am J Respir Crit Care Med*. 2000;161(2 Pt 1):581–588.
- [29] Denenberg VH: Some statistical and experimental considerations in the use of the analysis-of-variance procedure. *Am J Physiol*. 1984;246(4 Pt 2):R403–R408.
- [30] Truong-Tran AQ, Ruffin RE, Zaleski PD: Visualization of labile zinc and its role in apoptosis of primary airways epithelial cells and cell lines. *Am J Physiol Lung Cell Mol Physiol*. 2000;279:L1172–L1183.
- [31] Carter JE, Truong-Tran AQ, Grosser D, Ho L, Ruffin RE, Zaleski PD: Involvement of redox events in caspase activation in zinc-depleted airway epithelial cells. *Biochem Biophys Res Commun*. 2002;279:1062–1070.
- [32] Ho E, Courtemanche C, Ames BN: Zinc deficiency induces oxidative DNA damage and increases p53 expression in human lung fibroblasts. *J Nutr*. 2003;133:2543–2548.
- [33] Gomez NN, Fernandez MR, Zirulnik F, Gil E, Scardapane L, Ojeda MS, Gimenez MS: Chronic zinc deficiency induces an antioxidant adaptive response in rat lung. *Exp Lung Res*. 2003;29:485–502.
- [34] Gomez NN, Ojeda MS, Gimenez MS: Lung lipid composition in Zn-deficient rats. *Lipids*. 2002;37:291–296.
- [35] Cunnane SC, Yang J: Zn deficiency impairs whole-body accumulation of polyunsaturates and increases the utilization of [1-<sup>14</sup>C] linoleate for de novo lipid synthesis in pregnant rats. *Can J Physiol Pharmacol*. 1995;73:1246–1252.
- [36] King JC: Assessment of zinc status. *J Nutr*. 1990;120(Suppl 11):1474–1479.
- [37] Dorup I, Clausen T: Effects of magnesium and zinc deficiencies on growth and protein synthesis in skeletal muscle and the heart. *Br J Nutr*. 1991;66:493–504.
- [38] Maret W: Oxidative metal release from metallothionein via zinc-thiol/disulfide interchange. *Proc Natl Acad Sci U S A*. 1994;91:237–241.
- [39] Jacob C, Maret W, Vallee BL: Control of zinc transfer between thionein, metallothionein, and zinc proteins. *Proc Natl Acad Sci U S A*. 1998;95:3489–3494.
- [40] Dunn MA, Blalock TL, Cousins RJ: Metallothionein. *Proc Soc Exp Biol Med* 1987;185:107–119.
- [41] Lazo JS, Pitt BR: Metallothioneins and cell death by anticancer drugs. *Annu Rev Pharmacol Toxicol*. 1995;35:635–653.
- [42] Schwarz MA, Lazo JS, Yalowich JS, Allen WP, Whitmore M, Bergonia HA, Tzeng E, Billiar TR, Robbins PD, Lancaster JR, Pitt BR: Metallothionein protects against the cytotoxic and DNA-damaging effects of nitric oxide. *Proc Natl Acad Sci U S A* 1995;92:4452–4456.
- [43] Torres RL, Torres IL, Gamaro GD, Fontella FU, Silveira PP, Moreira JS, Lacerda M, Amoretti JR, Rech D, Dalmaz C, Belló AA: Lipid peroxidation and total radical-trapping potential of the lungs of rats submitted to chronic and sub-chronic stress. *Braz J Med Biol Res*. 2004;37:185–192.
- [44] Morrison D, Rahman I, Lannan S, MacNee W: Epithelial permeability, inflammation and oxidant stress in the air spaces of smokers. *Am J Respir Crit Care Med*. 1999;159:473–479.
- [45] Schwarzer C, Machen TE, Illek B, Fischer H: NADPH oxidase-dependent acid production in airway epithelial cells. *J Biol Chem*. 2004;279:36454–36461.
- [46] Bedard K, Krause KH: The NOX family of ROS-generating NADPH oxidases: physiology and pathophysiology. *Physiol Rev*. 2007;87:245–313.
- [47] Folz RJ, Abushama AM, Suliman HB: Extracellular superoxide dismutase in the airways of transgenic mice reduces inflammation and attenuates lung toxicity following hyperoxia. *J Clin Invest*. 1999;103:1055–1066.
- [48] Valko M, Izakovic M, Mazur M, Rhodes CJ, Telser J: Role of oxygen radicals in DNA damage and cancer incidence. *Mol Cell Biochem*. 2004;266:37–56.
- [49] Huie RE, Padmaja S: The reaction of NO with superoxide. *Free Radic Res Commun*. 1993;18:195–199.
- [50] Moriarty PM, Picciano MF, Beard JL, Reddy CC: Classical selenium-dependent glutathione peroxidase expression is decreased secondary to iron deficiency in rats. *J Nutr* 1995;125:293–301.
- [51] Corda S, Laplace C, Vicaute E, Duranteau J: Rapid reactive oxygen species production by mitochondria in endothelial cells exposed to tumor necrosis-alpha is mediated by ceramide. *Am J Respir Cell Mol Biol*. 2001;24:762–768.
- [52] Davis WB, Pacht ER, Spatafora M, Martin WJ 2nd: Enhanced cytotoxic potential of alveolar macrophages from cigarette smokers. *J Lab Clin Med* 1988;111:293–298.
- [53] Rahman I: Oxidative stress, transcription factors and chromatin remodelling in lung inflammation. *Biochem Pharmacol*. 2002;64:935–942.
- [54] Ricote M, Li AC, Willson TM, Kelly CJ, Glass CK: The peroxisome proliferator activated receptor-gamma is a negative regulator of macrophage activation. *Nature*. 1998;391:79–82.
- [55] Chung JJ, Cho S, Kwon YK, Kim DH, Kim K: Activation of retinoic acid receptor gamma induces proliferation of immortalized hippocampal progenitor cells. *Brain Res Mol Brain Res*. 2000;83:52–62.
- [56] Meerarani P, Reiterer G, Toborek M, Hennig B: Zinc modulates PPARgamma signaling and activation of porcine endothelial cells. *J Nutr*. 2003;133:3058–3064.
- [57] Govers R, Rabelink T J: Cellular regulation of endothelial nitric oxide synthase. *Am J Physiol Renal Physiol*. 2001;280:F193–F206.
- [58] Kobayashi K, Nishimura Y, Yamashita T, Nishiuma T, Satouchi M, Yokoyama M: The effect of overexpression of endothelial nitric oxide synthase on eosinophilic lung inflammation in a murine model. *Int Immunopharmacol*. 2006;6:1040–1052.
- [59] Gomez NN, Biaggio VS, Rozzen EJ, Alvarez SM, Gimenez MS: Zn-limited diet modifies the expression of the rate regulatory enzymes involved in phosphatidylcholine and cholesterol synthesis. *Br J Nutr*. 2006;96:1038–1046.
- [60] Thomas SR, Chen K, Keaney JF Jr: Hydrogen peroxide activates endothelial nitric oxide synthase through coordinated phosphorylation and dephosphorylation via a phosphoinositide 3-kinase-dependent signaling pathway. *J Biol Chem*. 2002;277:6017–6024.

- [61] Drummond GR, Cai H, Davis ME, Ramasamy S, Harrison DG: Transcriptional and posttranscriptional regulation of endothelial nitric oxide synthase expression by hydrogen peroxide. *Circ Res.* 2000;86:347–354.
- [62] Krein PM, Winston BW: Roles for insulin-like growth factor I and transforming growth factor- $\alpha$  in fibrotic lung disease. *Chest.* 2002;122 (6 Suppl):289S-293S.
- [63] Noble PW, Henson PM, Riches DW: Insulin-like growth factor-1 (IGF-1) mRNA expression in bone marrow derived macrophages is stimulated by chrysotile asbestos and bleomycin. A potential marker for a reparative macrophage phenotype. *Chest.* 1991;99 (3 Suppl):79S–80S.
- [64] Lefebvre D, Beckers F, Ketelslegers JM, Thissen JP: Zinc regulation of insulin-like growth factor-I (IGF-I), growth hormone receptor (GHR) and binding protein (GHBP) gene expression in rat cultured hepatocytes. *Mol Cell Endocrinol.* 1998;138:127–136.